Evaluation of different oxygen carriers for biomass tar reforming

2: Carbon deposition in experiments with methane and other gases

Mendiara, Teresa; Johansen, Joakim Myung; Utrilla, Rubén; Jensen, Anker Degn; Glarborg, Peter

Published in:
Fuel

Link to article, DOI:
10.1016/j.fuel.2010.12.034

Publication date:
2011

Evaluation of different oxygen carriers for biomass tar reforming (II): carbon deposition in experiments with methane and other gases

Teresa Mendiara *, Joakim M. Johansen, Rubén Utrilla, Anker D. Jensen and Peter Glarborg

Department of Chemical and Biochemical Engineering, Technical University of Denmark, 2800 Lyngby, Denmark

Abstract

This work is a continuation of a previous paper by the authors [1] which analyzed the suitability of the Chemical Looping technology in biomass tar reforming. Four different oxygen carriers were tested with toluene as tar model compound: 60% NiO / $MgAl_2O_4$ (Ni60), 40% NiO / $NiAl_2O_4$ (Ni40), 40% Mn_3O_4 / Mg-ZrO_2 (Mn40) and $FeTiO_3$ (Fe) and their tendency to carbon deposition was analyzed in the temperature range 873-1073 K. In the present paper, the reactivity of these carriers to other compounds in the gasification gas is studied, also with special emphasis on the tendency to carbon deposition. Experiments were carried out in a TGA apparatus and a fixed bed reactor. Ni-based carriers showed a tendency to form carbon in the reaction with CH_4, especially Ni60. The addition of water in H_2O/CH_4 molar ratios of 0.4-2.3 could decrease the carbon deposited, but not in the case of Ni60. Mn-based sample reacted with CH_4 almost completely and with low tendency to carbon deposition, while the Fe-based sample showed low reactivity. Ni40 showed more reactivity to CO than Mn40, although in both cases carbon was deposited,

especially at 873 K. When H_2 was present, it reacted rapidly with both carriers, decreasing the amount of carbon deposited. The presence of CO_2 could also decrease the carbon deposited on Ni40 at 1073 K. According to both these and the previous results [1], it can be concluded that Mn40 is the most adequate for minimization of carbon deposition in Chemical Looping Reforming (CLR).

Key words: biomass gasification, chemical looping, reforming, tar, toluene, methane

1 Introduction

In recent years, energy generation through biomass gasification has experienced an important development. The product gas formed from biomass gasification contains the major components CO, H_2, CO_2, CH_4, H_2O, and N_2, in addition to particulates, tars and inorganic impurities (H_2S, HCl, NH_3 and alkali metals). The final composition of the gas is influenced by many factors, including feed composition, water content, reaction temperature and the extent of oxidation of the pyrolysis products [2]. Also the gasifier configuration influences the composition. Most of the commercial gasifiers are downdraft, followed by fluidised bed and updraft gasifiers. Typical product gas concentrations for air-blown gasifiers are 9-17% H_2, 14-24% CO, 9-20% CO_2 and 1-7% CH_4 (% dry basis) [2].

The gasification gas obtained as a product may be fired directly or fed to an IC engine, gas turbine or fuel cell to produce electricity, along with heat in a CHP

* Corresponding author
Email address: tmendiara@icb.csic.es
Phone: +34 976 733 977
Fax: +34 976 733 318 (Teresa Mendiara).

system. Biomass gasification gas could also serve as a raw material for chemical synthesis. It can be used to produce methanol and hydrogen, or converted into synthetic fuel via the Fischer-Tropsch process. Each of these final applications set a limit in the degree of upgrading of the gas, which usually contains important amounts of undesirable tar [3]. Several techniques have been developed in order to both avoid the tar fouling operational problems and reach the tolerance levels of the different end-use devices or applications. The Chemical Looping Reforming technology (CLR) is among the newest approaches. In a companion paper by the authors, the suitability for tar elimination of this technology was analyzed [1]. The performance of four different oxygen carriers used in CL processes was studied using toluene (C_7H_8) as model compound for high temperature biomass tar. The analysis focused on the conditions to avoid or minimize carbon deposition from toluene. Ni40 and Mn40 presented interesting characteristics for CLR of biomass tar. Both showed stable reactivity to C_7H_8 after a few cycles. Ni40 showed a high tendency to carbon deposition, but could be controlled by decreasing the temperature and the time for the reduction step. The addition of water also reduced the amount of carbon deposited. Mn40 showed low tendency to form carbon when reacting with C_7H_8 both at 873 and 1073 K.

In the present work, the reactivity during the reforming process of some other species present in the gasification gas (CH_4, CO, H_2) is studied. Their final amount in the upgraded gas is important regarding further uses of it. Besides it is also interesting to analyze their contribution to carbon deposition. Carbon losses are not desiderable, not only regarding fouling problems but also considering further uses of the clean gas. Regarding this aspect, previous works have studied the carbon deposition in chemical looping processes when working with gases such as CH_4 and CO. In general, the carbon deposition on

a metal catalyst surface can be represented by the following reactions [4]:

$$2\,CO \overset{surf}{\rightleftharpoons} C(s) + CO_2 \tag{1}$$

$$CO + H_2 \overset{surf}{\rightleftharpoons} C(s) + H_2O \tag{2}$$

$$C_nH_{2n+2} \overset{surf}{\rightleftharpoons} n\,C(s) + (n+1)\,H_2 \tag{3}$$

The reactions (1) (Boudouard reaction) and (2) are favoured at low temperatures, lower than 650 °C for reaction (1) [5], while formation via reaction (3) becomes increasingly important at higher temperatures. Kinetically, both reaction (1) and (3) are known to have a limited importance in the absence of a catalyst.

Ishida et al. [6] investigated carbon deposition on oxygen carrier particles based on nickel and iron oxides with either YSZ, Al_2O_3 or TiO_2 as support at 600 °C in a TGA in the presence of CO. They suggested that the carbon formation was caused by the Bouduard reaction and found that the carbon deposition rates for iron-based particles were lower than for Ni-based particles except for Fe_2O_3/YSZ particles. For nickel oxide, the support affected the carbon deposition rate in the order Al_2O_3 > YSZ > TiO_2. They also studied the temperature effect in the interval 590-900 °C for the NiO/YSZ and found that, at 900 °C there was no carbon formation. The carbon deposits decreased with increased reaction temperature and H_2O/CO ratio.

Jin et al. [7] investigated carbon deposition on oxygen-carrier particles based on NiO with either YSZ or $NiAl_2O_4$ at 600 °C using a TGA with either methane or humidified methane as fuel. They found that the carbon deposition was caused by methane decomposition. However, the carbon formation was

completely avoided by adding water vapour at a ratio of H_2O/CH_4 of 2.

Ryu et al. [8] investigated the effects of different reaction temperatures on carbon deposition with a NiO/bentonite using a TGA. Methane diluted in nitrogen was used as the fuel in the temperature range 650-1000 °C. They showed that carbon formation decreased with increasing reaction temperature and, at temperatures above 900 °C, there was no carbon deposition.

Johansson et al. [9] compared two different Ni-based oxygen carriers: 60% NiO $/MgAl_2O_4$ and 40% $NiO/NiAl_2O_4$. Carbon deposition on the first carrier took place when the reaction products were mainly CO and H_2. On the contrary, carbon deposition on the second one was initiated very early in the solid reduction period even though the selectivity to CO_2 was very high . Nevertheless, neither of the particles managed to avoid carbon formation at CLR conditions.

Finally, Cho et al. [10] investigated the carbon formation on Ni and Fe-based oxygen carriers in a fluidized bed using CH_4 in the 750-950 °C temperature range. The Ni-based oxygen carrier clearly catalyzed the carbon formation to the largest extent. Carbon formation was strongly dependent on the availability of oxygen. Independently of either steam addition or temperature, when more than 80% of the available oxygen was consumed, rapid formation of carbon was started. For the particles with iron oxide no or very little carbon was formed, even when the conversion of the fuel was very low.

In this paper and as a continuation of the previous work by the authors [1], the reaction of the same oxygen carriers with CH_4, CO and H_2 (in the presence of H_2O and CO_2) will be studied. The main focus will be on the influence on carbon formation of temperature, in the range 873-1073 K, and H_2O/C_xH_y molar ratio, with the aim of determining the conditions to avoid or minimize

the carbon deposition. Considering also the previous results with C_7H_8, the present findings could be used to suggest the most adequate oxygen carrier for low carbon deposition in CLR of biomass tar.

2 Experimental

2.1 Oxygen carriers

The composition, preparation method and some of the properties of the four carriers tested can be found in Table 1. For a better clarity and throughout this paper, the reference name for each of them will be used. Ni60 represents the oxygen carrier with 60% NiO supported on $MgAl_2O_4$. Ni40 contains 40% NiO on $NiAl_2O_4$. In Mn40, the active phase is the mixed-oxide Mn_3O_4, which constitutes 40% weight of the carrier and is supported on Mg-ZrO_2. Finally, Fe represents the natural ore ilmenite ($FeTiO_3$). Prior to any test, ilmenite was oxidized to its most oxidized state for 24 h at 1223 K in a 1 dm^3/min (STP) air stream [11].

The maximum amount of oxygen that may be transferred from the carriers is given by their oxygen capacity (R_0), defined as:

$$R_0 = \frac{m_{ox} - m_{red}}{m_{ox}} \tag{4}$$

where m_{ox} and m_{red} are the mass of the sample when it is fully oxidized or reduced, respectively. The R_0 values for the four samples are: Ni60 (0.126), Ni40 (0.086), Mn40 (0.028) and Fe (0.05).

The Ni-based carriers have been tested before for both Chemical Looping Combustion (CLC) and CLR applications [9, 12–17]. Johansson et al. [9] and Zafar et al. [17] found that a fully Ni60 reduced sample was never achieved and that the active material in Ni60 was 50%. This difference was related to the reaction of active and carrier material during heat treatment with formation of compounds such as MgO, $MgNiO_2$ and $NiAl_2O_4$ [15, 17, 18]. Ni60 turned out to be better than Ni40 at converting methane, as it had been previously reported [14, 15, 19]. The reactivity of Ni60 to methane was highly dependent on temperature and displayed a large increase between 800 and 1000 °C [17]. Furthermore, a large increase in reactivity was also found in experiments with syngas between 650 and 950 °C. On the other hand, earlier experiments with Ni40 and CH_4 at different temperatures showed no significant increase in reactivity between 750 and 950 °C [16]. The suitability of Ni60 and Ni40 for CLR of CH_4 has been analyzed previously by Johansson et al. [9].

The Mn-based carrier (40% Mn_3O_4/Mg-ZrO_2) has been tested both in CLC [20] and CLR [21] conditions. Mn-based carrier was found to perform better in CLC, but its reforming behaviour at the lower temperatures of this study has not been analyzed. Finally, ilmenite ($FeTiO_3$) has been used recently in CLC of both gaseous fuels (CH_4, syngas) [22, 23] and several solid fuels (coke, charcoal, lignite, bituminous coal [11, 24]. Ilmenite showed good properties in CLC at high temperatures (around 970 °C) but no previous testing of its reforming properties has been carried out.

2.2 Experimental setups

The reactivity of the four carriers to the major components of the biomass gasification gas (CH_4, CO, H_2O, H_2 and CO_2) was analyzed according to the five gaseous systems showed in Table 2. Their concentrations were set similar to the ones present in a real gasification gas. The presence of toluene (C_7H_8), as model tar compound, was also considered in some of the systems. Two different setups have been used in the study, a thermogravimetrical analysis apparatus (TGA) and a fixed bed reactor (FB).

2.2.1 Thermogravimetric analysis device (TGA)

The four different carriers were tested in different atmospheres in a thermogravimetric apparatus Netzsch STA 409 C. Table 3 shows the experiments performed at atmospheric pressure in the range 873-1073 K.

Oxygen carrier particles were sieved to a size of 180-212 μm. In all the experiments, 10 mg of carrier particles were well-spread at the bottom of an alumina crucible forming a single layer, in order to avoid the interparticle mass transfer resistance. The weight changes in the sample were registered by a highly sensitive analytical balance located in the casing of the apparatus. Around 100 cm^3/min (STP) purge N_2 were always introduced to the balance chamber to maintain the inert atmosphere, while the total flow to the reactor chamber was set to 150 cm^3/min (STP).

In a similar way as it was done in the experiments with C_7H_8 [1], the sample was subjected to reaction at different temperatures consecutively (873-1073-873 K). At each temperature, the sample was exposed in a cyclic manner to a

reducing atmosphere and to a mixture of O_2 and N_2. Different gaseous mixtures were tested in the reducing period: CH_4, CH_4 + H_2O, and CH_4 + C_7H_8 + H_2O. In the experiments with CH_4 and H_2O, two different H_2O/CH_4 molar ratios were analyzed. They were obtained by saturation of a 50 cm^3/min (STP) nitrogen-diluted CH_4 stream with H_2O at 313 and 333 K, respectively. In the cases in which C_7H_8 was also fed, the CH_4 stream was saturated with C_7H_8 at 270.5 K before being saturated with water. During the oxidizing period, the particles were regenerated in the presence of O_2 diluted in N_2. For Ni60, Ni40 and Mn40, the duration of the cycles were 9 minutes for reduction and 8 min for oxidation; in the case of the Fe sample, it was 30 and 25 min, respectively. Five/eight reducing-oxidizing cycles were carried out at each temperature. Nitrogen was introduced between reducing and oxidizing steps during 3 minutes to avoid mixing gaseous atmospheres.

2.2.2 Fixed bed reactor (FB)

Table 4 presents the gaseous systems investigated in the FB experiments, only for the Ni40 and Mn40 samples. A quartz fixed bed reactor was used. The reactor was 17 mm internal diameter and 610 mm in length, with a porous plate in the middle (90-150 μm pore size). Solid particles in the size range 212-250 μm were used. In every experiment, 400 mg of sample were placed on a thin quartz wool bed on the plate.

The reactor was located inside an electrically heated oven. Prior to the reactivity tests, the temperature profiles in the reactor were measured at non-reacting conditions. The four oxygen carriers were tested in a temperature range 873-1073 K. The reactor pressure (around 0.11 MPa) was measured by a manometer connected to the inlet line. A control panel connected to mass

flow controllers was used to prepare the mixture of gases to be fed to the reactor. Toluene was fed by saturating a N_2 stream at 288 K. The water was fed to the system by saturating a N_2 flow with H_2O at 343-348 K in an evaporator. The total reactant gas flow to the reactor was maintained at 2.0 dm^3/min (STP). The dry composition of the cooled gas was analyzed through a continuous gas analyzer. A Rosemount NGA 2000 MLT gas analyzer determined the concentration of O_2 (paramagnetic), CO and CO_2 (infrared). The accuracy in the measured concentration was below or equal to 1% of the measurement range, and the typical measurement ranges were set to be 0-10% for O_2, 0-20% for CO and 0-25% CO_2. All data from each experiment (temperature, pressure and concentrations as a function of time) were logged in a file.

The samples experienced consecutive reducing and oxidizing cycles. The duration of the cycles were 4 minutes for reduction and 3 minutes for oxidation. Four/five cycles were performed with each sample. A nitrogen flow cleaned the reactor during 2 minutes between the reducing and subsequent oxidizing step. After each experiment, the sample was taken out of the reactor by removing the bottom part of it.

3 Results and discussion

The discussion of the results will be presented considering the systems in Table 2. The objective was to first test the reactivity to some of the main gasification gases alone (or in the presence of H_2O) and secondly, test the performance of the carriers under different gaseous mixtures resembling the gasification gas. The reactivity to CH_4 and CO are analyzed in systems A (A.1 and A.2) and C (C.1 and C.2), respectively. System B studies the behaviour when both

CH_4 and C_7H_8 are present in the gaseous stream. The results can give an idea about the conditions where carbon deposition is minimized. System D is a combination of system B and system C and system E tries to reproduce the composition of a real gasification gas, where CO_2 is also present and can contribute to the final amount of carbon deposited.

3.1 Reactivity with CH_4

3.1.1 Thermogravimetrical analysis

Thermogravimetrical experiments were performed to analyze the reactivity of the four different oxygen carriers to CH_4 with and without the presence of H_2O. Diffusion limitations due to the actual TGA configuration were proven not to affect the present results [1].

Dry CH_4

The experiments for the reactivity of the different carriers to CH_4 without the presence of water (system A.1 in Table 2) were conducted following a temperature ramp 873-1073-873 K. First, the evolution with time of the weight loss in the reduction step with the number of cycles was investigated. Ni60 presented no reactivity to CH_4 in the first set of experiments at 873 K (not shown). An increase in temperature to 1073 K resulted in an increase in reactivity. Figure 1 (A) shows the weight loss for the 1^{st}, 4^{th} and 8^{th} cycle at this temperature. It is clearly seen that the weight loss increases with the number of cycles while the carbon deposition on the sample decreases. The maximum weight loss value is 5.5 %, which represents around 44% of the oxygen transfer

capacity of the carrier (R_0). In the TGA experiments, the weight loss observed during the reduction period might be the result of both the reduction of the carrier and carbon deposition, two competing processes that could take place at the same time. During the 3 minute flushing period, only N_2 was introduced in the TGA reactor chamber. Nevertheless, a slight decrease in the sample weight is observed. As it has been reported earlier [9, 10, 15], since there is no other oxygen source than the oxygen on the particles present at that stage, the following solid-solid reaction could take place:

$$C + M_yO_x \longrightarrow CO/CO_2 + M_yO_{x-1/2} \tag{5}$$

where M_yO_x represents the oxygen carrier. When oxygen is introduced, the carbon deposited is burned off and the carrier is re-oxidized fast. There are no important differences in the oxidation rates observed in the different cycles with Ni60 at 1073 K. After reacting at 1073 K, a new set of cycles at 873 K is carried out. In this condition, Ni60 reacted with CH_4 as shown in Figure 1 (B). The activation of the carrier after reacting at higher temperatures in the same atmosphere has been observed before in experiments with C_7H_8 and H_2O [1] and this result is quite interesting regarding the practical operation with this carrier. As it was observed at higher temperature, the weight loss increases with the number of cycles while the final carbon deposition decreases. The maximum weight loss corresponds in this case to 40% of R_0. No weight loss during the inert period was observed at 873 K (2^{nd} set) and the oxidation rates for the different cycles were similar.

Ni40 reacted both at 873 (1^{st} and 2^{nd} set) and 1073 K with CH_4. For all the temperatures tested, only a slight increase in the weight loss with the number

of cycles was observed. The weight loss was stable after 4 cycles. In the first set of experiments at 873 K (not shown), some carbon was deposited on the carrier and its reoxidation was not complete, specially in the first cycle. The maximum weight loss represented around 70% of the oxygen transfer capacity. Figure 1 (C) shows the weight loss for the 1^{st}, 4^{th} and 8^{th} cycle at 1073 K. The amount of carbon deposited on the carrier decreased significantly and the maximum weight loss increased to around 88% of the value of R_0. The carrier did not completely re-oxidize, but the oxidation rates are similar in the different cycles. In the final set at 873 K in Figure 1 (D), the behaviour of the carrier was similar to the observed in the first set. In this case, the maximum weight loss was around 73% of R_0. This value is higher than the one observed in the first set at 873 K, which indicates a slight activation effect of the carrier after reacting at 1073 K.

Both Mn40 and Fe reacted with CH_4 only at the highest temperature tested (1073 K). Figure 1 (E) shows the weight loss for the 1^{st}, 4^{th} and 8^{th} cycle at 1073 K. For Mn40, no increase in weight loss during the reducing period suggests the absence of carbon deposition in these conditions. In all the cases, the final weight loss corresponded to the oxygen transfer capacity (R_0), although the weight loss rate was slower in the first cycle compared to the rest. The reoxidation rate of the carrier was similar for all the cycles and the carrier re-oxidized completely. The behaviour of Fe is shown in Figure 1 (F). Almost no reactivity to CH_4 was observed in any of the cycles.

According to these results, the samples with higher tendency to carbon deposition in the reaction with CH_4 are Ni60 and Ni40. This tendency was analyzed in more detail in experiments in which the samples, after two preliminary reducing/oxidizing cycles, reacted with 6.67% CH_4 at 1073 K during 2 hours,

so that the evolution of carbon deposition on the carrier could be traced with time. The weight increase registered for Ni60 was much more pronounced than for Ni40. After the two hour experiment, the weight of the Ni60 sample had increased around 25 % compared to its initial value. This confirmed previous findings of Johansson et al. [9], which also showed important deposition on Ni60 when reacting with CH_4. Carbon was deposited on Ni40, but at a much slower rate. Mn40 and Fe showed no sign of carbon deposition when subjected to the same conditions. Similar results working with CH_4 and Mn_3O_4 were obtained before [25].

All the samples were observed after reaction by Scanning Electron Microscopy (SEM). Figure 2 (A) shows first the images obtained for the fresh Ni60 sample. Spherical particles of the oxygen carrier are observed, as it may be expected from the freeze granulation preparation method used. Figure 2 (B) shows the particles after reaction with methane. The particles have been broken down and their shape is far from spherical. The porosity seems to have increased compared to the fresh particles. Figure 2 (C) shows the reduced particles in more detail. Long and thin filaments could be seen arising from the carrier particles. These structures are carbon whiskers and their formation and characteristics have been extensively analyzed in many hydrocarbon reforming studies [26, 27]. Dissolution of carbon in nickel is essential to the growth of carbon whiskers [4]. Once the carbon has dissolved and formed a compound with nickel (Ni_3C), diffusion through the metal particle to a grain boundary occurs. Carbon precipitates out and lifts the nickel particle at the tip of a growing whisker.

The Ni40 sample was also observed by SEM, but in this case no significant changes in the carrier morphology were detected. Previous studies have indi-

cated that the carbon deposited on the $NiO/NiAl_2O_4$ particle was elemental carbon and no nickel carbides were formed [7]. Actually, not all the coke formed on the surface dissolves in nickel [4]. Some carbon may remain on the surface and encapsulate nickel. In experiments with CH_4, Jin et al. [7] observed that the $NiO/NiAl_2O_4$ particle was swollen by the deposited carbon and was broken into small fragments. The growth of carbon whiskers depend on the nucleation of carbon somewhere inside the metal zones, such as grain boundaries. Nuclei growth will eventually push the metal particles out of the surface. However, if carbon can also nucleate and grow on the surface without difussing into the bulk carbon, encapsulation will occur [28].

SEM images of both Ni-based carriers point to different carbon formation mechanisms on Ni60 and Ni40. Regarding the higher rate of carbon deposition on Ni60, we attribute it to the larger size of the Ni nanocrystallites in Ni60 compared to Ni40. Larger crystallites yield larger chance for carbon formation [29]. However, Transmission Electron Microscopy (TEM) studies of both used Ni samples are required to confirm this hypothesis.

A high concentration of hydrogen in the reducing gas may also favour the formation of carbon whiskers [28]. This could be the case of the Ni60 experiment with CH_4. The higher NiO load compared to Ni40 would favour methane reforming catalyzed by Ni and therefore a high H_2 concentration in the gas. Besides, the consumption of the H_2 generated by the remaining NiO would not be favoured, as it is known that the carriers with the addition of magnesium were less good at oxidizing H_2 [9]. In the experiment with CH_4 and Ni40, the support ($NiAl_2O_4$) would also contribute to a lower rate of carbon formation. It has been previously reported that $NiAl_2O_4$ is more stable not to promote carbon deposition [30]. Finally, the SEM images obtained for Mn40

and Fe samples did not show any significant morphological difference with the original samples.

Wet CH_4

Previous studies underlined the reduction in the amount of carbon deposited when increasing the value of the H_2O/CH_4 molar ratio [7]. In the present work, the four oxygen carriers were tested in the reaction with CH_4 and two different H_2O/CH_4 molar ratios, i.e. 0.4-1 (system A.2 in Table 2). Figures 3 to 5 compare the weight loss curves versus time in the 8^{th} cycle for the experiment where no water was present and the experiments with different amounts of H_2O.

Figure 3 shows the results for the Ni60 sample at different temperatures. Although the opposite was expected, the addition of H_2O in the experiments with Ni60 resulted in an increase of carbon deposition at all the temperatures tested, although there are no significant differences in the increment value registered for the two different H_2O/CH_4 ratios. At 1073 K (top), the carbon deposited increases the sample weight from around 95% to 97%, while in the case without water it changed from 94.5% to 95.7%. Even more explicit was the difference in the experiments at 873 K (2^{nd} set) (bottom). In the experiment without water, the weight changed from 94.9 to 97.3%, while in the experiments under the water presence the change was around 95.5 to 98.5%. At 1073 K, the amount of carbon deposited seems to be linearly related to the reaction time. At 873 K (2^{nd} set), two different carbon deposition rates are observed, with faster values in the beginning of the carbon deposition period.

In literature, carbon deposition is mainly attributed to the Bouduard reac-

tion, reaction (1), and hydrocarbon decomposition (CH_4 in this case), reaction (3). Methane decomposition is an endothermic reaction, thermodynamically favored at high temperatures whereas the Bouduard reaction is exothermic and more likely to take place at lower temperatures. Therefore, at 873 K, the carbon deposition may be caused by both the methane decomposition and, specially, Bouduard reaction. At the moment at which carbon deposition overcomes the rest of the reactions taking place, the carrier has transferred an important part of the oxygen. In these conditions, it might be possible that the partial oxidation of the fuel occurs, leading to the formation of CO and H_2.

$$CH_4 + NiO \longrightarrow CO + 2\,H_2 + Ni \tag{6}$$

The CO formed decomposes rapidly according to the Bouduard reaction, but once the oxygen carrier has been almost completely reduced, no more CO is produced, and the carbon deposited is caused by methane decomposition. The change in the predominant carbon deposition mechanism could explain the two carbon deposition rates observed at 873 K in the experiment without H_2O. The fast region would correspond to the fast CO decomposition favoured at low temperatures and the slow one, almost unnoticeable, to the contribution of methane decomposition when no more CO is produced by the partial oxidation of the carrier. In the experiments with H_2O, the steam methane reforming reaction, reaction (7), catalyzed by Ni, leads to CO production,

$$CH_4 + H_2O \rightleftharpoons CO + 3\,H_2 \tag{7}$$

The additional CO produced decomposes according to the favoured Bouduard

reaction and contributes to carbon deposition even when the carrier has been completely reduced and CO from the partial oxidation of the carrier is not generated. This contribution to carbon deposition would explain the steady increase in the weight sample after the fast carbon deposition region in the experiments with H_2O at 873 K.

At 1073 K, the amount of carbon formed via the Boudouard reaction is very low compared to the amount deposited by methane decomposition, around 20 times less at 1050 K [31]. In both experiments with and without H_2O, carbon formation is mainly caused by the methane decomposition which would explain the steady increase with time of the amount deposited.

It is also interesting to note that there are only slight differences in the maximum weight loss registered at the beginning of the experiments with respect to the case with no water. Besides, the reduction time without carbon deposition increased when the H_2O/CH_4 ratio in the feed increased, which is in agreement with data reported in literature at high temperature range (800-950 °C) [32]. In all the experiments, the carrier was re-oxidized to its original state.

The effect of H_2O addition on the experiments with Ni40 and CH_4 is depicted in Figure 4. Again, almost no difference is observed in the value of the maximum weight loss compared to the maximum value without water, and the reduction time without carbon deposition increases when H_2O/CH_4 ratio increases, specially at 873 K (1^{st} and 2^{nd} set) (top and bottom). Nevertheless, the H_2O addition does not lead to a carbon deposition enhancement similar to the observed with the Ni60 sample. In the experiment without water at 873 K (both sets), the two carbon deposition regions with different deposition rates can be observed. However, the additional CO produced in the H_2O experi-

ments through reaction (7) does not increase carbon deposition in the second region as much as it was observed with the Ni60 sample. Only at the highest H_2O/CH_4 ratio (value equal to 1) a slight increase is observed, considering that the sensitivity of the TGA apparatus is 1.25 μg. At 1073 K (middle), water addition does not increase carbon deposition. On the contrary, a slight decrease, higher than 1.25 μg, is observed for the two H_2O/CH_4 molar ratios tested. The amount of carbon formed is small compared to the experiments at 873 K, as it can be deduced from the little weight loss registered at the beginning of the oxidizing period.

Finally, Figure 5 shows the corresponding weight loss-time curves at 1073 K for the experiments with Mn40, in Figure 5 (A) and with Fe, in Figure 5 (B). In the case of Mn40, the addition of water does not affect the reaction with CH_4, as the weight loss is almost identical with and without H_2O in both reducing and oxidizing periods in the experiments. The presence of H_2O in the Fe experiments with CH_4 seems to activate the carrier. Independently of the H_2O/CH_4 ratio used, the carrier registers a weight loss to around 98%, compared to the drop to 99.5% in the case without H_2O. It is interesting to note that, as ilmenite is a natural ore, it may not be porous. An increase in porosity may take place with the alternate reducing-oxidizing periods and therefore, the reactivity will increase with sucessive cycles. This fact has been also outlined in recent publications where ilmenite was tested under several reducing-oxidizing cycles with different fuels [33].

3.1.2 Fixed bed reactor

The analysis of the reactivity of the carriers with CH_4 was completed with some FB experiments in order to compare the trends found in the TGA for

Ni40 and Mn40. The conditions are presented in Table 4. In the FB experiments, the reaction temperature is the same through the whole experiment. The concentrations of CO, CO_2 and O_2 were measured for the reduction and oxidation step of each cycle. An example of the concentration profiles obtained in a typical experiment are shown in Figure 6. Those measurements were used to extract information about carbon deposition during the process as it was described elsewhere [1].

The moles of carbon deposited were calculated from the CO and CO_2 concentrations during the oxidizing step:

$$C_{deposited} = F_{oxi} \cdot \int_{t_0}^{t_{oxi}} (C_{CO_{oxi}} + C_{CO_{2,oxi}}) dt \tag{8}$$

where $C_{CO_{oxi}}$ and $C_{CO_{2,oxi}}$ are CO and CO_2 concentrations in the outlet stream and F_{oxi} is the molar flow in the oxidizing period.

In a similar way, the moles of carbon released as CO and CO_2 in the reducing period were calculated:

$$C_{reducing} = F_{red} \cdot \int_{t_0}^{t_{red}} (C_{CO_{red}} + C_{CO_{2,red}}) dt \tag{9}$$

where $C_{CO_{red}}$ and $C_{CO_{2,red}}$ are CO and CO_2 concentrations in the outlet stream and F_{red} is the molar flow in the reducing period.

Finally, the moles of oxygen that were transferred by the carrier during the reducing period were estimated as:

$$O_{reacted} = F_{oxi} \cdot \int_{t_0}^{t_{oxi}} (2 \cdot (C_{O_{2,0}} - C_{O_2}) - (C_{CO_{oxi}} + 2 \cdot C_{CO_{2,oxi}}))dt \qquad (10)$$

where $C_{O_{2,0}}$ is the initial oxygen concentration in the gas stream and C_{O_2} the oxygen concentration at different times.

These values were used in the calculation of the following parameters:

- Percentage of carbon deposited in the reducing step (C_{dep})

$$C_{dep} = \frac{C_{deposited}}{C_{introduced}} \cdot 100 \qquad (11)$$

- Solid conversion in the reducing step (X_O)

$$X_O = \frac{O_{reacted}}{O_{introduced}} \qquad (12)$$

- Carbon conversion in the reducing step (X_c)

$$X_c = \frac{C_{deposited} + C_{reducing}}{C_{introduced}} \qquad (13)$$

Dry CH_4

Figure 7 compares the evolution of the carbon deposition percentage and the solid conversion in the experiments of (A) Ni40 and (B) Mn40 with CH_4 and no H_2O. The carbon deposited on the Ni40 in Figure 7 (A) decreases in the second cycle and remains more or less stable in the rest of the 5 cycles. The percentage of carbon deposited is slightly higher at 873 K, which is in agreement with the TGA findings in the same conditions. The solid conversion is also stable from the second cycle. Its value is close to 0.9 at 1073 K and around 0.6 at 873 K. The global carbon conversion in the reducing step,(X_c),

has also been calculated. The values stabilize quickly after the second cycle and remain close to 6% in the experiments at 1073 K and to 4.5% at 873 K. This means that the amount of carbon reacted is around 3.5 and 2 times the amount of carbon deposited at 1073 and 873 K, respectively. Figure 7 (B) shows the results obtained for Mn40. As it was observed in the TGA experiments, Mn40 shows a high reactivity at 1073 K, with high solid conversion, close to the maximum, and almost no carbon deposition (0.14% of the carbon introduced). The carbon conversion (X_c) was around 0.8%, which means that the amount of carbon reacted in the reducing step was around 4.5 times the amount of carbon deposited. At 873 K, no reactivity was observed at any of the sets of experiments done in the TGA. In the FB experiments, the reactivity shown by the carrier was very low.

Wet CH_4

The configuration used in the fixed bed experiments allowed testing higher H_2O/CH_4 molar ratios than those used in the TGA experiments. In this case, the molar ratios varied between 1.5 and 2.3. Figure 8 shows the effect of water addition at 1073 K for Ni40. Similarly to the results in the TGA experiments, the amounts of carbon deposited and the solid conversion rapidly become stable with the number of cycles. At 1073 K, the addition of water reduces the amount of carbon deposition. This reduction is higher with the lowest H_2O/CH_4 tested (1.5). Water also increases the values of the carbon conversion to 57.5% and 64% for the molar ratios 1.5 and 2.3, respectively, which may indicate that the CH_4 reforming reaction takes place in a considerable extent. The values of the solid conversion are similar for the experiments with and without water, also in agreement with the TGA results.

The study of the reactivity to CH_4 of the four different carriers showed that Ni60 had a high tendency to carbon deposition and it was even enhanced with the addition of water, specially at 873 K. Ni40 led also to carbon deposition, but not in that great extent. At 1073 K, the amount deposited could even be reduced by the addition of water. Mn40 and Fe showed no tendency to carbon deposition at any temperature. The Fe sample only showed some reactivity to CH_4 at 1073 K and the reaction rate was low compared to its maximum oxygen transfer capacity, R_0 (0.05). However, in previous experiments with C_7H_8 as model tar compound [1], Fe showed very little reactivity to this hydrocarbon. Considering all of this, the use of Ni60 and Fe as oxygen carriers in a CLR process was disregarded and therefore, in the following, only Ni40 and Mn40 will be considered for a further study of the reactivity of the carriers in different gaseous atmospheres.

A thermodynamic study about carbon formation using fuels present in a common biomass gasification gas was performed for the Ni-based sample (Ni40), as it showed the highest tendency to carbon deposition both in experiments with CH_4 and C_7H_8 [1]. For the thermodynamical calculations, the software HSC Chemistry 6.1 was used [34]. This software finds the most stable phase combination and determines the phase composition where the Gibbs energy of the system reaches its minimum value at a fixed balance, constant pressure and temperature.

The oxygen ratio to avoid carbon formation as a function of temperature was calculated, as it was done in previous studies [35]. The oxygen ratio is defined as the oxygen reacted with the fuel with respect to the stoichiometric amount

of oxygen needed to reach complete fuel conversion. The values of the oxygen ratio in the 873-1073 K temperature range have been represented in Figure 9 for CH_4 and several combinations of gases present in the biomass gas that can lead to carbon deposition. This gaseous mixtures are CH_4 + C_7H_8 and CH_4 + C_7H_8 + CO, where the molar ratio were $CH_4/C_7H_8 \approx 28$ and CH_4/CO ≈ 0.33, similar to the values used afterwards in the experiments summarized in Tables 3 and 4. When only CH_4 is present, the value of the oxygen ratio decreases with temperature and for the highest temperature tested (1073 K) reaches a value of 0.25. When the mixture CH_4 + C_7H_8 was analyzed, the same trend with temperature was observed, but the presence of C_7H_8, although not in high proportion respect to CH_4, contributed to increase the value of the oxygen ratio needed to avoid carbon formation. Finally, in the mixture containing CO and both hydrocarbons, the effect of CO on the oxygen ratio is clear. At low temperatures, the value of the oxygen ratio increases notably, because Bouduard reaction (reaction 1) is favoured in these conditions. As temperature increases, the contribution of this reaction to carbon deposition decreases.

Considering these results, the experiments named under system B in Table 2 will be presented first. The reactivity of the two aforementioned carriers to both CH_4 and C_7H_8 is analyzed in the presence of water. The objective is to compare the reaction of the hydrocarbon mixture with Ni40 and Mn40 to the reaction with the hydrocarbons individually in the same experimental conditions.

3.2.1 Thermogravimetrical analysis

The TGA experiments were performed using the temperature ramp 873-973-873 K. The reason for this has been presented earlier [1]. At temperatures higher than 973 K and with or without the presence of water, the C_7H_8 decomposition in the gas phase takes place due, mainly, to the high residence time of the reacting gas in the TGA reaction chamber. This phenomenon leads to the formation of pyrolytic carbon and soot [36].

In the first set at 873 K, there was no reaction between Ni40 and the mixture of hydrocarbons, contrary to the results with CH_4 or C_7H_8 alone. Figure 10 (A) compares the Ni40 weight loss with time in experiments with only CH_4, only C_7H_8 and with both of them, in the presence of water and for the second set at 873 K. The weight loss in the experiment with both hydrocarbons is slightly higher than that observed in the experiment with CH_4, although the time of the reduction period where carbon deposition starts to be the dominant process is lower than in the case of CH_4. The carbon deposition increases with time during the whole reducing period and the final amount is also higher than in the case of the experiment with CH_4. According to these results, CH_4 reacts fast with the carrier, consuming almost all the oxygen present. When the carrier is almost completely reduced, the contribution of C_7H_8 to carbon deposition is significant. During the inert period, a slight decrease in the sample weight is observed, which suggests that reaction (5) may be taking place. The reoxidation of the carrier is different to that observed in the CH_4 experiment. The oxidation of the carbon deposited is much slower, as the subsequent reoxidation of the carrier, which does not reach the initial weight. The incomplete regeneration of the carrier was also observed in the experiment with only C_7H_8. This could suggest that the kind of carbon deposited in the

reaction with CH_4 is different from the one formed in the reaction with only C_7H_8. At 973 K (not shown), there was also carbon deposition on the almost depleted carrier when reacting with the hydrocarbon-water mixture.

Mn40 reacted with the hydrocarbon-water mixture at 873 K (both sets), while there was no reaction at 873 K when reacting with only CH_4. Figure 10 (B) shows the weight losses when reacting in similar conditions with each hydrocarbon individually at 873 K (2^{nd} set). The weight loss in the experiment with both hydrocarbons is slightly lower than in the experiment with only toluene. This may indicate a competition between the reaction of the carrier with C_7H_8 and CH_4 and the reforming/carbon formation on the already reduced carrier. Nevertheless, no final carbon deposition was detected during the oxidizing period and the reoxidation rate of the carrier was similar to the case with only C_7H_8. At 973 K, some carbon deposition was observed in the experiment with the mixture.

3.2.2 Fixed bed reactor

The FB experiments allowed for experiments with Ni40 and Mn40 at higher temperatures than in the TGA, i.e in the 873-1073 K range. The residence time of the reactant gases in the reaction zone was much lower than in the TGA and this prevented toluene from thermal cracking. Also in FB experiments, different C_7H_8 concentrations were tested (0.25 and 0.74 %), which corresponds to H_2O/C_7H_8 molar ratios of 63.6 and 21.1, respectively. The H_2O/CH_4 molar ratio was maintained to 2.3. As before, the concentrations of CO, CO_2 and O_2 were measured for each cycle. From those measurements, the percentage of carbon deposited (C_{dep}) and the solid conversion (X_O) in each cycle were calculated.

Effect of temperature

The carbon deposition percentage and the solid conversion in the experiments of Ni40 and Mn40 with CH_4, C_7H_8 and H_2O at 1073 and 873 K is compared in Table 5. For C_7H_8 and a concentration of 0.25%, the percentage of carbon deposited on Ni40 increases with temperature. The solid conversion is rather low at 873 K, maybe due to the reoxidation of the carrier by H_2O at this low temperature. The solid conversion increases notably with temperature. In the case of Mn40, the amount of carbon deposited is low, almost neglibible at 873 K. This tendency to a higher carbon deposition at higher temperatures might be due again to higher C_7H_8 decomposition at higher temperatures.

Effect of toluene concentration

It was considered interesting to analyze the effect of an increase in the amount of toluene introduced to the system at the highest temperature, i. e. when toluene decomposition is favoured. This analysis could estimate the effect on the carbon deposited of the changes in the amount of tar present in the feeding gas. Table 5 shows the effect of an increase in C_7H_8 concentration from 0.25% to 0.75 % at 1073 K for both Ni40 and Mn40. For Ni40, the percentage of carbon deposited increased dramatically, approximately 6.5 times, and a slight reduction in the solid conversion was observed. In the case of Mn40, the increment in the same conditions was around 1.7 times, but the amount deposited remained at low levels.

3.3 Reactivity to CO and mixtures CO/H_2

System C in Table 2 analyzes the reactivity of the selected carriers, Ni40 and Mn40, with CO and the mixture CO and H_2. The study of this system will give some knowledge about CO contribution to carbon deposition and also CO consumption, as its preservation may be interesting for further uses in chemical synthesis processes.

Carbon deposition is observed in the CO experiments in Table 6 for Ni40 and Mn40, both at 873 and 1073 K. For Ni40, the percentage of carbon deposited decreased with the increase in temperature from 1.42% at 873 K to 1.02% at 1073 K, which supports the increase in carbon deposition in the TGA experiments with CH_4 at 873 K when H_2O was present, compared to the case with no H_2O. When water was present, CH_4 reforming would lead to an increase in the CO concentration. This CO would decompose according to Boudouard reaction, favored at low temperatures as seen in this Table, and would increase the carbon deposited (Figure 4). The solid conversion in the experiments with CO increased with temperature up to a value of 0.55 at 1073 K. The values of carbon conversion (X_c) for the 5^{th} cycle were around 4.26% at 873 K and 4.75% at 1073 K, so the amount of carbon reacted was around 2 and 3.75 times the amount of carbon deposited at 873 and 1073 K, respectively. The effect of the addition of H_2 on CO reaction with Ni40 could also be seen in Table 6. When H_2 was present, the amount of carbon deposited decreased and the solid conversion increased to values around 0.7 (873 K) and 0.8 (1073 K). The carbon conversion (X_c) values in the last cycle were 3.3 and 3.6 % at 873 and 1073 K, respectively, and therefore the ratio of carbon reacted to carbon deposited changed to 2.6 at 873 K and 3.5 at 1073 K when

H_2 was added.

In this case, the reactions taking place in the reducing period were the CO and H_2 oxidation to CO_2 and H_2O,

$$CO + NiO \longrightarrow CO_2 + Ni \tag{14}$$

$$CO + Mn_3O_4 \longrightarrow CO_2 + 3\,MnO \tag{15}$$

$$H_2 + NiO \longrightarrow H_2O + Ni \tag{16}$$

$$H_2 + Mn_3O_4 \longrightarrow H_2O + 3\,MnO \tag{17}$$

together with CO decomposition following Bouduard reaction (reaction 1).

$$2\,CO \overset{surf}{\rightleftharpoons} C(s) + CO_2$$

The solid conversion incresases compared to the experiments with only CO, due to the H_2 reaction with the carrier. Besides, the observed reduction in the amount of carbon deposited in comparison with CO experiments may be due to the carbon gasification by the water produced in hydrogen oxidation. The process is represented by the reverse of reaction 2:

$$CO + H_2 \overset{surf}{\rightleftharpoons} C(s) + H_2O$$

Mn40 shows low reactivity to CO at the temperatures tested, although carbon deposition was observed, more or less to the same extent (around 1%) at both 873 and 1073 K. In this temperature range the sample mainly reacts with H_2, and carbon deposition diminishes due to its gasification by the produced H_2O.

System D combines in one gaseous mixture the gases present in system B and system C.2., i.e. the gaseous mixture consists of CH_4, C_7H_8, H_2O, CO and H_2. In the case of Ni40, a decrease in the carbon deposited with temperature was observed in system D, while the tendency was the opposite in the experiments with only CH_4, C_7H_8 and H_2O (system B). This decrease in carbon deposited may be due to the presence of H_2 in the gas. Higher solid conversions than in system B were also observed both for Ni40 and Mn40.

Finally, system E analyzes the reactivity of the selected carriers, Ni40 and Mn40, with a gaseous mixture similar to the biomass gasification gas composition, i. e. CH_4, C_7H_8, H_2O, CO, H_2 and CO_2. The presence of CO_2 could contribute to enhance the dry reforming reactions and, therefore, reduce the amount of carbon deposited in the system:

$$C_nH_m + n\,CO_2 \rightleftharpoons 2n\,CO + 1/2m\,H_2 \tag{18}$$

To facilitate the comparison between the two carriers, the percentage of carbon deposited has been normalized in Figure 11 considering the oxygen capacity, R_0, of the Ni40 and Mn40 samples. The normalized value for carbon deposition is much higher in the case of Ni40 than in the case of Mn40 for all the temperatures tested (12 times at 873 K and 4.5 at 1073 K). Therefore, in the real CLR process, Ni40 is expected to lead to a greater carbon deposition than Mn40. Nevertheless, the trend in the carbon deposition evolution with temperature is different for the two carriers. The normalized value of carbon deposition decreases with temperature in the case of Ni40, probably due to a

higher extent in the reaction of the carrier with H_2 but also to the contribution to carbon deposition reduction of the dry reforming process. However, in Mn40 a slight increase of the normalized value with temperature is observed. The value at 1073 K is around 1.4 times the value at 873 K. Regarding the carrier conversion, values around 0.62 at 873 K and 0.75 at 1073 K were observed for Ni40. For Mn40 varied between 0.87 at 873 K and 0.81 at 1073 K.

4 Practical implications

The combination of both the results in the previous paper by the authors [1] and the present results could give some recommendations in order to select the right oxygen carrier for CLR of biomass tar from the four tested. First of all, the carrier should present reactivity to C_7H_8 used as a biomass tar model compound in this study. According to this, Ni60 should be discarded as it did not show any reactivity in the temperature range 873-1073 K. Fe should be disregarded as well, because although it presented some reactivity, the very low reaction rate would necessitate high solid circulation in a real system. The remaining carriers, Ni40 and Mn40 showed high reactivity to C_7H_8 at the different temperatures tested.

A strong tendency to carbon deposition when reacting with other carbonaceous species, such as CH_4 or CO, represents an important drawback when considering one carrier as potential material for the CLR process. Besides the operational problems which might occur, the excessive carbon deposition could lead to a significant loss of carbon in the system when the carrier is regenerated in the air reactor. This is not desirable, especially when the gasification gas is planned to be used as raw gas for chemical synthesis. These

considerations reinforce discarding Ni60 as suitable CLR carrier, as it showed high tendency to deposit carbon in the reaction with CH_4, even enhanced in the presence of water.

Ni40 reacted with CH_4 and carbon was deposited. This amount of carbon was notably reduced when water was present and then, CH_4 reforming consumed great part of the CH_4 introduced, specially at 1073 K. In the reaction with C_7H_8 carbon deposition was also observed on Ni40 and the amount increased with temperature. Water addition decreases carbon deposition. However, the value of the ratio H_2O/C_7H_8 should be selected carefully in order to avoid reoxidation of the carrier when high concentrations of water were present. Besides, the C_7H_8 concentration in the feeding gas had a great influence in the amount of carbon deposited. Ni40 also reacted with CO, leading to carbon deposition, specially at 873 K. When H_2 was present, it reacted rapidly with the carrier in the temperature range tested and favoured the decrease in the amount of carbon deposited. The presence of CO_2 could also help to decrease the carbon deposited at high temperatures by dry reforming reactions.

Mn40 did not react with CH_4 at 873 K but it did with C_7H_8 in the 873-1073 K, with a lower tendency to carbon deposition when compared to Ni40. The carbon deposited in the reaction with C_7H_8 could be decreased by the addition of H_2O in the right concentration to avoid carrier re-oxidation. Again at 873 K, Mn40 did not almost show reactivity to CO, although it reacted with H_2.

To sum up, at 873 K, Mn40 does not react significantly with either CH_4 or CO, only with C_7H_8 with low tendency to carbon deposition which can be minimized by the addition of water. This complies with the objectives of minimization of the carbon loss in the system and preservation of CH_4 and CO for further use. Therefore and according to the present experimental

indications, Mn40 could be the best choice for CLR oxygen carrier.

5 Concluding remarks

The reaction between four oxygen carriers and different gaseous atmospheres typical of biomass gasification gas was analyzed. The conditions for carbon deposition in the different systems were investigated. In some cases, the experiments were performed in both a TGA and a FB reactor.

- In the experiments with CH_4, Ni60 reactivity at the lowest temperature tested (873 K) was affected by a previous pretreatment at highest temperatures. The rest of the carriers, either they were not affected in that great extent (Ni40) or they were not affected at all (Mn40 and Fe). Ni40 and Mn40 reactivity became stable quickly with the number of cycles, specially at high temperatures. Fe showed reactivity to CH_4 only at 1073 K an it was very low. This reactivity increased with the number of cycles and with the addition water. Regarding carbon deposition, Ni60 showed a high tendency to carbon formation when reacting with CH_4 and this was enhanced with the addition of water specially at the lowest temperature. Ni40 formed carbon, but not in that great extent. At 1073 K, the amount deposited could even be reduced by the addition of water. Mn40 and Fe showed no tendency to carbon formation at any temperature.
- In experiments with both CH_4 and C_7H_8 carbon deposition was not completely avoided in spite of the high H_2O/C_xH_y molar ratio used in the case of Ni40. It increased slightly with temperature, probably due to the C_7H_8 contribution. There were indications that the kind of carbon formed from CH_4 was not the same as the formed from C_7H_8. An increase in C_7H_8 con-

centration resulted, in the case of Ni40, in an important increase in the percentage of carbon deposited.

- Ni40 reacts with CO at both 1073 and 873 K. Carbon deposition is observed, more at the lowest temperature, i. e. 873 K. Mn40 showed low reactivity to CO in this temperature range. The presence of H_2 in the reaction of CO with both Ni40 and Mn40 decreased the amount of carbon deposited.
- The presence of CO_2 in the reacting gaseous mixture could contribute to reduce carbon deposition on Ni40 through dry reforming at the highest temperature tested (1073 K).

6 Acknowledgments

This project is part of the Era-Net Bioenergy project *Energy efficient selective reforming of hydrocarbons*. The authors thank the funding received from Energinet.dk.

References

[1] Mendiara T, Johansen JM, Utrilla R, Geraldo P, Jensen AD, Glarborg P. Evaluation of different oxygen carriers for biomass tar reforming (I): carbon deposition in experiments with toluene. Fuel;2010. In press. DOI: 10.1016/j.fuel.2010.11.028

[2] Bridgwater T, Biomass for energy. J Sci Food Agric 2006;86:1755-68.

[3] Milne TA, Evans RJ, Abatzoglou N. Biomass gasifier "tars": their nature, formation and conversion. NREL Report NREL/TP-570-25357. Colorado; 1998.

[4] Trimm DLA. Catalysts for the control of cocking during steam reforming. Catal Today 1999;49:3-10.

[5] Świerczyński D, Courson C, Kiennemann A. Study of steam reforming of toluene used as model compound of tar produced by biomass gasification. Chem Eng Process 2008;47:508-13.

[6] Ishida M, Jin H, Okamoto T. Kinetic behaviour of solid particles in chemical-looping combustion: suppressing carbon deposition in reduction. Energy Fuels 1998;12:223-29.

[7] Jin H, Okamoto T, Ishida M. Development of a novel chemical-looping combustion: synthesis of a solid looping material of $NiO/NiAl_2O_4$. Ind Eng Chem Res 1999;38:126-32.

[8] Ryu Ho-J, Lim N-Y, Bae D-H, Jin GT. Carbon deposition characteristics and regenerative ability of oxygen carrier particles for chemical-looping combustion. Korean J Chem Eng 2003;20:157-62.

[9] Johansson M, Mattisson T, Lyngfelt A, Abad A. Using continuous and pulse experiments to compare two promising nickel-based oxygen carriers for use in chemical-looping technologies. Fuel 2008;87:988-1001.

[10] Cho P, Mattisson T, Lyngfelt A. Carbon formation on nickel and iron oxide-containing oxygen carriers for chemical-looping combustion. Ind Eng Chem Res 2005;44:668-76.

[11] Leion H, Mattisson T, Lyngfelt A. Solid fuels in chemical-looping combustion. Int J Greenhouse Gas Control 2008;2:180-93.

[12] Johansson M, Mattisson T, Lyngfelt A. Use of $NiO/NiAl_2O_4$ particles in a 10kW chemical-looping combustor. Ind Eng Chem Res 2006;45:5911-19.

[13] Johansson M, Mattisson T, Lyngfelt A. Comparison of oxygen carriers for chemical-looping combustion. Therm Sci 2006;10:93-107.

[14] Johansson M, Mattisson T, Lyngfelt A, Thunman H. Combustion of syngas and natural gas in a 300 W chemical-looping combustor. Chem Eng Res Des 2006;89:819-27.

[15] Mattisson T, Johansson M, Lyngfelt A. The use of NiO as an oxygen carrier in chemical-looping combustion. Fuel 2006;85:736-47.

[16] Mattisson T, Johansson M, Jerndal E, Lyngfelt A. The reaction of $NiO/NiAl_2O_4$ particles with alternating methane and oxygen. Can J Chem Eng 2006;86:756-67.

[17] Zafar Q, Abad A, Mattisson T, Gevert B. Reaction kinetics of freeze-granulated $NiO/MgAl_2O_4$ oxygen carrier particles for chemical-looping combustion. Energy Fuels 2007;21:610-18.

[18] Zafar Q, Mattisson T, Gevert B. Redox investigation of some oxides of transition-state metals Ni, Cu, Fe and Mn supported on SiO_2 and $MgAl_2O_4$. Energy Fuels 2006;20:34-44.

[19] Villa R, Cristiani C, Groppi G, Lietti L, Forzatti P, Cornaro U, Rossini S, Ni based oxide materials for CH_4 oxidation under redox cycle conditions. J Mol Catal A: Chem 2003:204-205:637-46.

[20] Abad A, Mattisson T, Lyngfelt A, Rydén M. Chemical-looping combustion in a 300 W continuously operating reactor system using manganese-based oxygen carrier. Fuel 2006;85:1174-85.

[21] Rydén M, Lyngfelt A, Mattisson T, Chen D, Holmen A, Bjørgum E. Novel oxygen carrier materials for chemical-looping combustion and chemical-looping reforming; $La_xSr_{1-x}Fe_yCo_{1-y}O_{3-\delta}$. Int J Greenh Gas Con 2008;2:21-36.

[22] Leion H, Lyngfelt A, Johansson M, Jerndal E, Mattisson T. The use of ilmenite as an oxygen carrier in chemical-looping combustion. Chem Eng Res Des 2008;86:1017-26.

[23] Leion H, Mattisson T, Lyngfelt A. Use of ores and industrial products as oxygen carriers in chemical-looping combustion. Energy Fuels 2009;23:2307-15.

[24] Leion H, Jerndal E, Steenari B-M, Hermansson S, Israelsson M, Jansson E, Johnsson M, Thunberg R, Vadenbo A, Mattisson T, Lyngfelt A. Solid fuels in chemical-looping combustion using oxide scale and unprocessed iron ore as oxygen carriers. Fuel 2009;88:1945-54.

[25] Stobbe ER, de Boer BA, Geus JW. The reduction and oxidation behaviour of manganese oxides. Catal. Today 1999;47:161-67.

[26] Rostrup-Nielsen JR, Tottrup PB. In: Proceedings of the Symposium in Science of catalysis and its applications in industry, Paper 39, Sindri (India); 1979.

[27] Helveg S, Lopez-Carles C, Sehested J, Hansen PL, Clausen BS, Rostrup-Nielsen RJ, Abild-Pedersen F, Nørskov JK. Atomic-scale imaging of carbon nanofibre growth. Nature 2004;427:426-29.

[28] La Cava AI, Bernardo CA, Trimm DL. Studies of deactivation of metals by carbon deposition. Carbon 1982;20:219-23.

[29] Rostrup-Nielsen JR. Steam reforming. In: Ertl G, Knözinger H, Schüth F, Weitkamp J, editors. Handbook of heterogeneous catalysis, 2^{nd} edition, Wiley-VCH; 2008, p. 2882-2905.

[30] Numaguchi T, Kikuchi K. Deactivation of bimodal nickel catalyst for steam methane reforming reaction. Ind. Eng. Chem. Res. 1991;30:447-53.

[31] Claridge JB, Green MLH, Tsang SC, York APE, Ashcroft AT, Battle PD. A study of carbon deposition on catalyst during the partial oxidation of methane to synthesis gas. Catal Lett 1993;22:299-305.

[32] de Diego LF, Ortiz M, Adánez J, García-Labiano F, Abad A, Gayán P, Synthesis gas generation by chemical-looping reforming in a batch fluidized bed reactor using Ni-based oxygen carrier. Chem Eng J 2008;144:289-98.

[33] Adanez J, Cuadrat A, Abad A, Gayán P, de Diego LF, García-Labiano F. Ilmenite activation during consecutive redox cycles in chemical-looping combustion. Energy Fuels 2010;24:1402-13.

[34] HSC Chemistry 6.1, Chemical reaction and equilibrium software with with thermochemical database and simulation module; Oututec Research Oy, Pori, Finland, 2008.

[35] Adánez J, Dueso C, de Diego LF, García-Labiano F, Gayán P, Abad A. Effect of fuel gas composition in chemical-looping combustion with Ni-based oxygen carriers. 2. Fate of light hydrocarbons. Ind Eng Chem Res 2009;48:2509-18.

[36] Bruinsma OSL, Geertsma RS, Bank P, Moulijn JA, Gas phase pyrolysis of coal-related aromatic compunds in a coiled tube flow reactor. Fuel 1988;67:327-33.

Tables

Table 1
Main characteristics of the oxygen carriers

Reference Name	**Ni60**	**Ni40**	**Mn40**	**Fe**
Composition	60% NiO	40% NiO	40% Mn_3O_4	94.3% $FeTiO_3$
	40% $MgAl_2O_4$	60% $NiAl_2O_4$	60% Mg-ZrO_2	
Production	FG[a]	FG[a]	FG[a]	Mineral
Calcination T / K	1673	1873	1423	-
Particle density / kg m^{-3}	3200	3800	2260	3600
Porosity	0.42	0.36	0.58	—
BET surface area / m^2 g^{-1}	1.24	0.4	—	0.11
Oxygen capacity (R_0) w/w	0.129	0.086	0.028	0.05

[a] FG: Freeze granulation

Table 2
Gaseous systems analyzed

System	**Gases**[b]	**TGA**	**FB**
A	**A.1** CH_4	X	X
	A.2 $CH_4 + H_2O$	X	X
B	$CH_4 + C_7H_8 + H_2O$	X	X
C	**C.1** CO	-	X
	C.2 $CO + H_2$	-	X
D	$CH_4 + C_7H_8 + H_2O + CO + H_2$	-	X
E	$CH_4 + C_7H_8 + H_2O + CO + H_2 + CO_2$	-	X

[b] Diluted in N_2

Table 3
TGA experiments with the different oxygen carriers and gaseous atmospheres

System[c]	**Sample**	**T / K**	**[Fuel]**	**[Fuel] / %**	$\mathbf{H_2O/C_xH_y}$	$\mathbf{N}_{cycles}$
A	All	873 - 1073 - 873	CH_4	6.67	0	24
	All	873 - 1073 - 873	CH_4 + H_2O	6.67	0.4 - 1	24
B	Ni40, Mn40	873 - 973 - 873	CH_4 + C_7H_8 + H_2O	6.67/0.25/6.67	1/26.4	15

[c] t_R (reduction) = 9; (Fe) 30 minutes; [O_2] = 6.67 % ; t_O (oxidation) = 8; (Fe) 25 minutes

Table 4
FB experiments with the different oxygen carriers and gaseous atmospheres

System [d]	**[Fuel]**	**[Fuel] / %**	$\mathbf{H_2O/C_xH_y}$	$\mathbf{N}_{cycles}$
A.1	CH_4	6.9	0	5
A.2	CH_4 + H_2O	6.9	1.5 - 2.3	5
B	CH_4 + C_7H_8 + H_2O	6.8/0.25-0.74/15.7	2.3/63.6-21.1	5
C.1	CO	20.3	0	5
C.2	CO + H_2	20.2/11.9	0	5
D	CH_4 + C_7H_8 + H_2O + CO + H_2	6.7/0.24/15.5/19.8/11.7	2.3/63.5	5
E	CH_4 + C_7H_8 + H_2O + CO + H_2 + CO_2	6.8/0.25/16.1/20.1/11.9/7.6	2.4/64.9	4

[d] Samples: Ni40, Mn40
Parameters: T = 873 - 1073 K; t_R (reduction) = 4 minutes; $[O_2]$ = 4 % ; t_O (oxidation) = 3 minutes

Table 5
Carbon deposition percentage and solid conversion (5^{th} cycle) in the system B experiments of Ni40 and Mn40 at different temperatures and C_7H_8 concentrations, t_R = 4 minutes

Carrier	**T / K**	**[C_7H_8]** / %	**C_{dep} / %**	**X_0**
Ni40	1073	0.25	0.88	0.70
		0.74	5.85	0.57
	873	0.25	0.54	0.02
Mn40	1073	0.25	0.11	0.85
		0.74	0.19	0.79
	873	0.25	0.00	0.07

Table 6
Carbon deposition percentage and solid conversion (5^{th} cycle) in the system C experiments of Ni40 and Mn40 at different temperatures, $t_R = 4$ minutes

Carrier	**System**	**T / K**	**C_{dep} / %**	**X_0**
Ni40	C.1	1073	1.02	0.55
		873	1.42	0.19
	C.2	1073	0.81	0.82
		873	0.92	0.74
Mn40	C.1	1073	1.00	0.02
		873	1.04	0.08
	C.2	1073	0.02	1.04
		873	0.04	1.00

List of Figure Captions

Fig. 1 Comparison of the weight loss with time for the 1^{st}, 4^{th} and 8^{th} cycle in the experiments of (A)-(B) Ni60 (C)-(D) Ni40 (E) Mn40 and (F) Fe with CH_4 (6.67%) at different temperatures. Times for reduction (R), purge (P) and oxidation (O) periods have been indicated by vertical dashed lines

Fig. 2 SEM pictures of the Ni60 sample (A) fresh, (B)-(C) after 120 minutes reaction with CH_4 (6.67%) without the presence of H_2O at 1073 K

Fig. 3 Weight changes versus time in the 8^{th} reduction step in the Ni60 reaction with CH_4 (6.67%) and different H_2O/CH_4 molar ratios (W) at (A) 1073 K and (B) 873 K (2^{nd} step). Times for reduction, purge and oxidation periods have been indicated by vertical dashed lines

Fig. 4 Weight changes versus time in the 8^{th} reduction step in the Ni40 reaction with CH_4 (6.67%) and different H_2O/CH_4 molar ratios (W) at (A) 873 K (1^{st} step) (B) 1073 K and (C) 873 K (2^{nd} set). Times for reduction, purge and oxidation periods have been indicated by vertical dashed lines

Fig. 5 Weight changes versus time in the 8^{th} reduction step in the (A) Mn40 and (B) Fe reaction with CH_4 (6.67%) and different H_2O/CH_4 molar ratios (W) at 1073 K. Times for reduction, purge and oxidation periods have been indicated by vertical dashed lines

Fig. 6 Example of raw data from a FB experiment: CO, CO_2 and O_2 evolution during Ni40 reaction with CH_4 (6.67%) at T = 1073 K. Times for reduction (R), purge (P) and oxidation (O) periods have been indicated by vertical dashed lines in the 3^{rd} cycle

Fig. 7 Comparison of the carbon deposition percentage and solid conversion evolution in the experiments of (A) Ni40 and (B) Mn40 with CH_4 (6.9%) and no H_2O at different temperatures, t_R (reduction) = 4 minutes. The filled symbols correspond to the highest temperature (1073 K) and the empty symbols to 873 K. The square-marked lines represent carbon deposition percentage and the circles, solid conversion

Fig. 8 Comparison of the carbon deposition percentage and solid conversion evolution in the experiments of Ni40 with CH_4 (6.9%) with different H_2O/CH_4 molar ratios (W) at 1073 K, t_R (reduction) = 4 minutes. The square-marked lines represent carbon deposition percentage and the circles, solid conversion

Fig. 9 Thermodynamic limit for carbon formation as a function of the oxygen ratio and temperature. Molar ratios $CH_4/C_7H_8 \approx 28$ and $CH_4/CO \approx 0.33$

Fig. 10 Comparison of (A) Ni40 and (B) Mn40 weight loss as a function of time in the 5^{th} cycle for CH_4 + H_2O, C_7H_8 + H_2O and CH_4 + C_7H_8 + H_2O experiments at 873 K (2^{nd} set); $[CH_4]$ = 6.67%, $[C_7H_8]$ = 0.25%, $[H_2O]$ = 6.67%. Times for reduction, purge and oxidation periods have been indicated by vertical dashed lines

Fig. 11 Comparison of the carbon deposition percentage per gram of oxygen introduced (5^{th} cycle) in the system E experiments of Ni40 and Mn40 at different temperatures, t_R (reduction) = 4 minutes

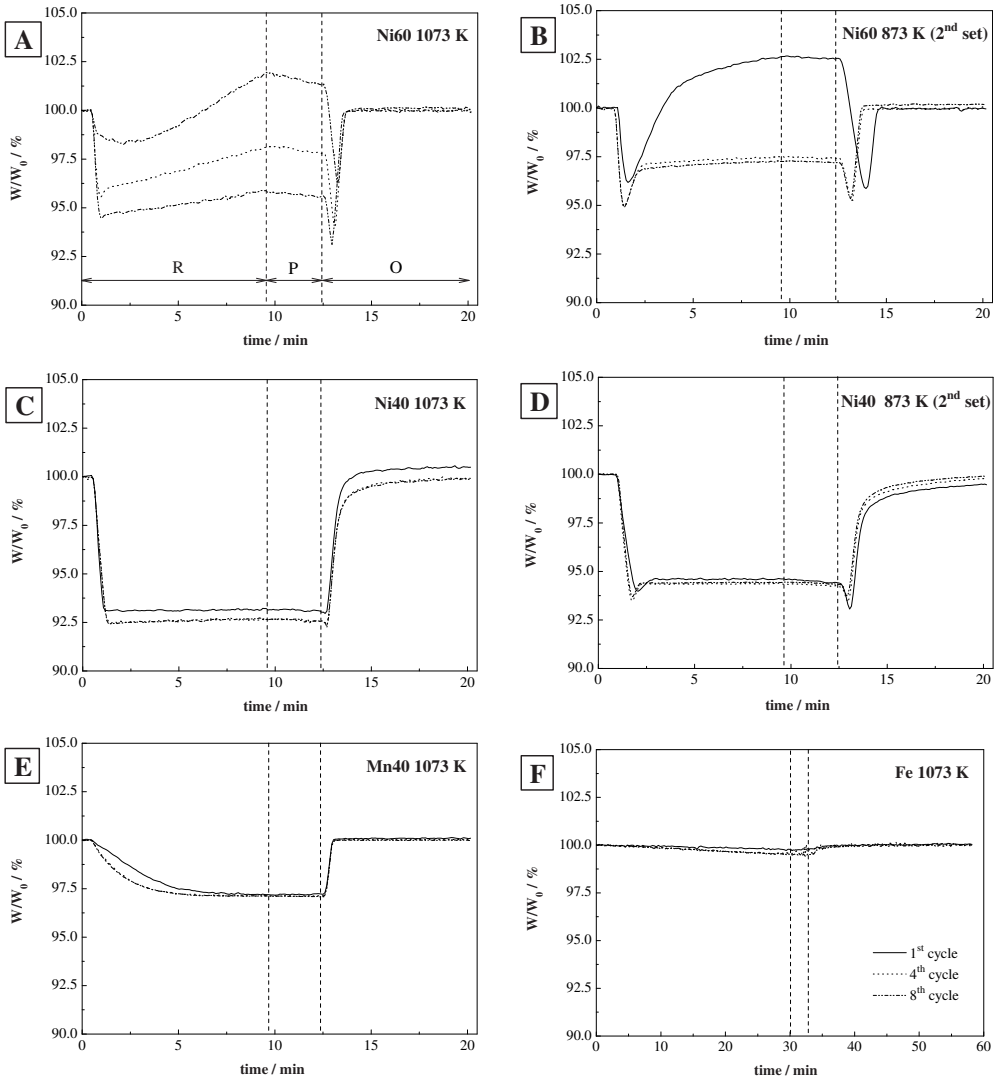
A
Ni60 1073 K
B
Ni60 873 K (2nd set)
C
Ni40 1073 K
D
Ni40 873 K (2nd set)
E
Mn40 1073 K
F
Fe 1073 K
R
P
O
W/W0 / %
time / min
1st cycle
4th cycle
8th cycle

Fig. 1.

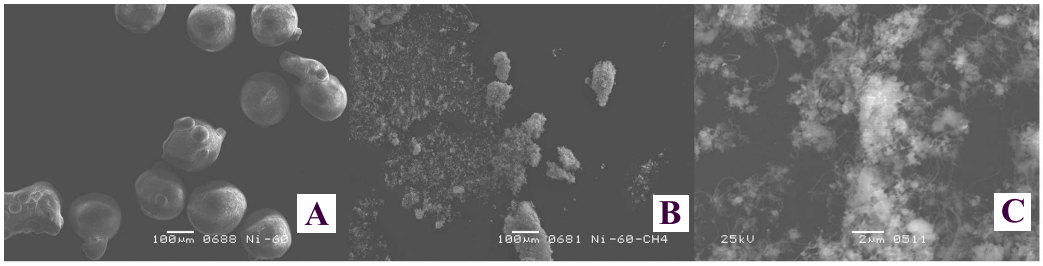

Fig. 2.

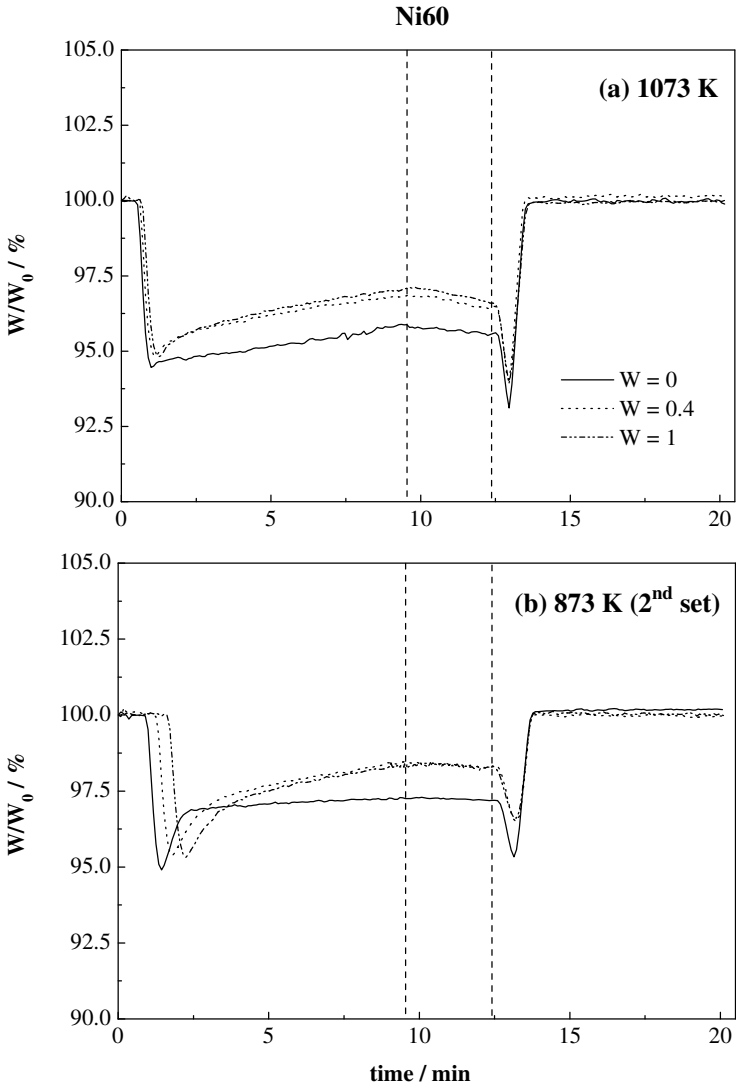
Ni60
(a) 1073 K
W = 0
W = 0.4
W = 1
(b) 873 K (2nd set)
W/W0 / %
time / min
105.0
102.5
100.0
97.5
95.0
92.5
90.0
0
5
10
15
20

Fig. 3.

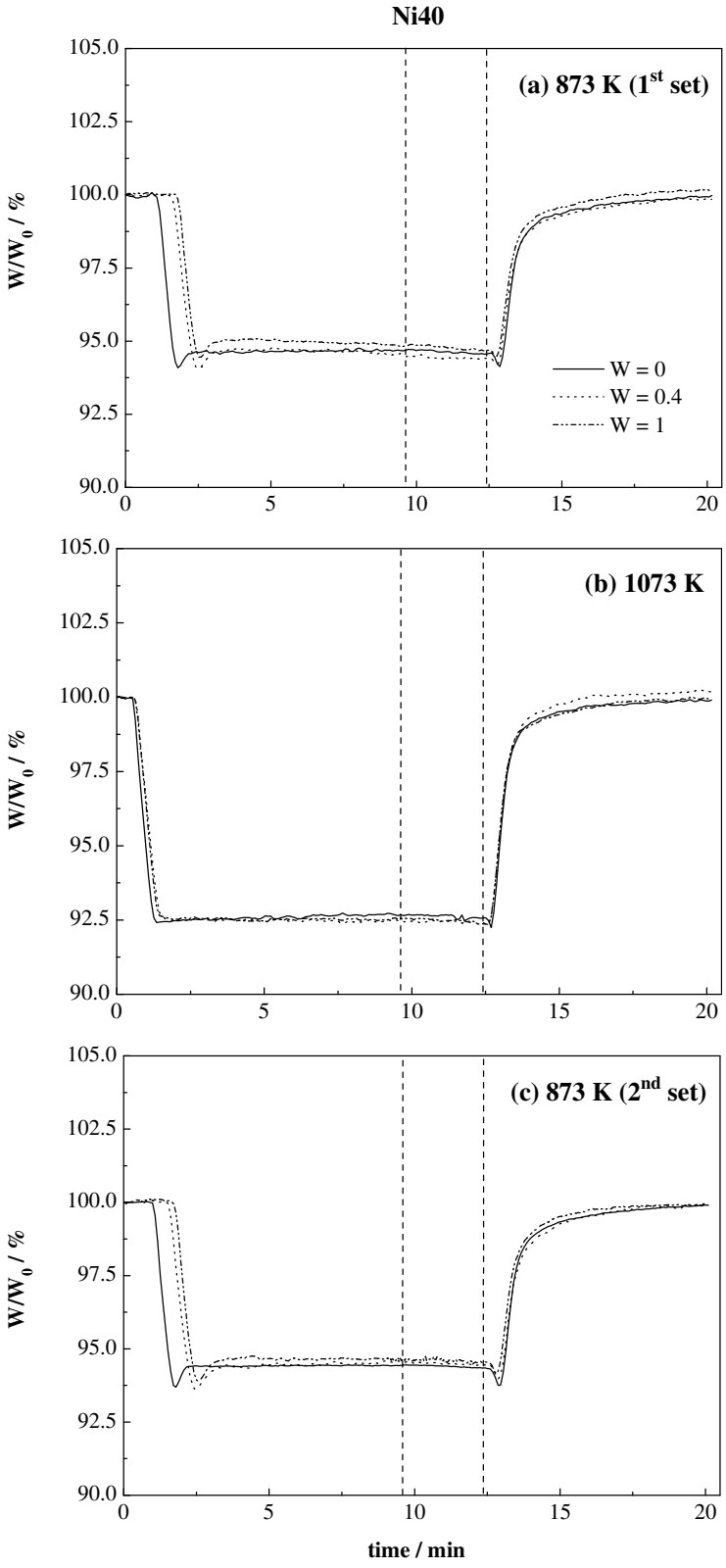
Ni40
(a) 873 K (1st set)
(b) 1073 K
(c) 873 K (2nd set)
W = 0
W = 0.4
W = 1
W/W0 / %
time / min
105.0
102.5
100.0
97.5
95.0
92.5
90.0
0
5
10
15
20

Fig. 4.

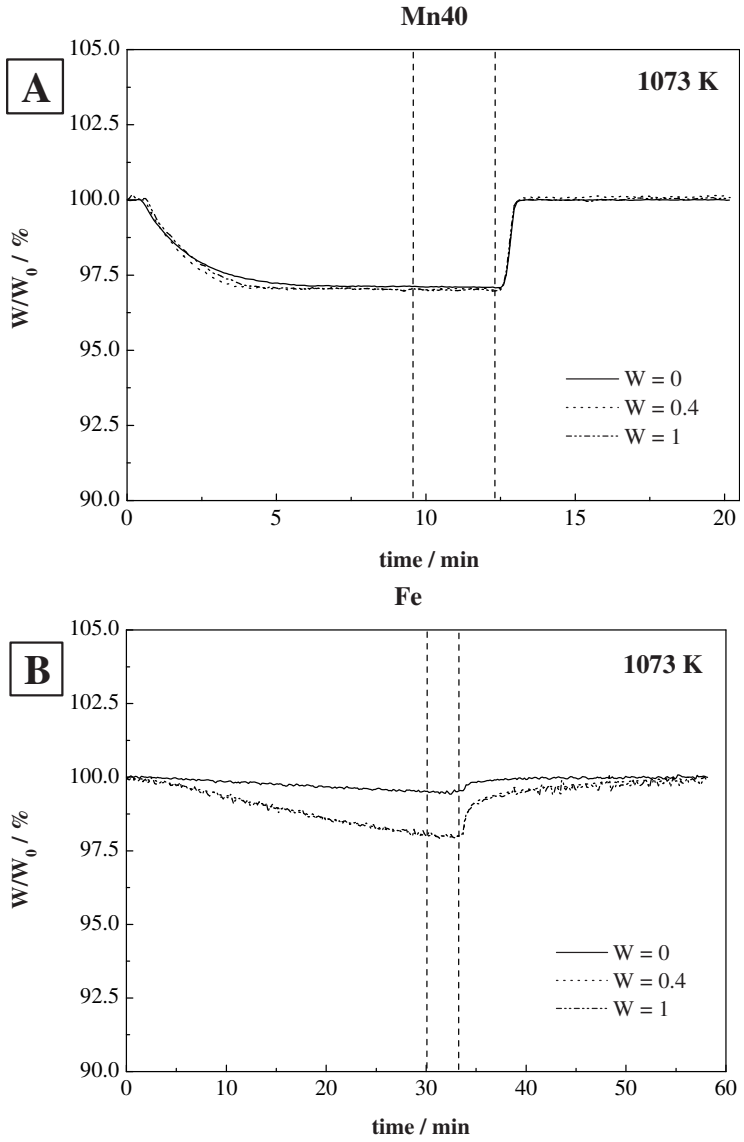
Mn40
A
1073 K
105.0
102.5
100.0
97.5
95.0
92.5
90.0
W/W0 / %
0
5
10
15
20
time / min
W = 0
W = 0.4
W = 1
Fe
B
1073 K
105.0
102.5
100.0
97.5
95.0
92.5
90.0
W/W0 / %
0
10
20
30
40
50
60
time / min
W = 0
W = 0.4
W = 1

Fig. 5.

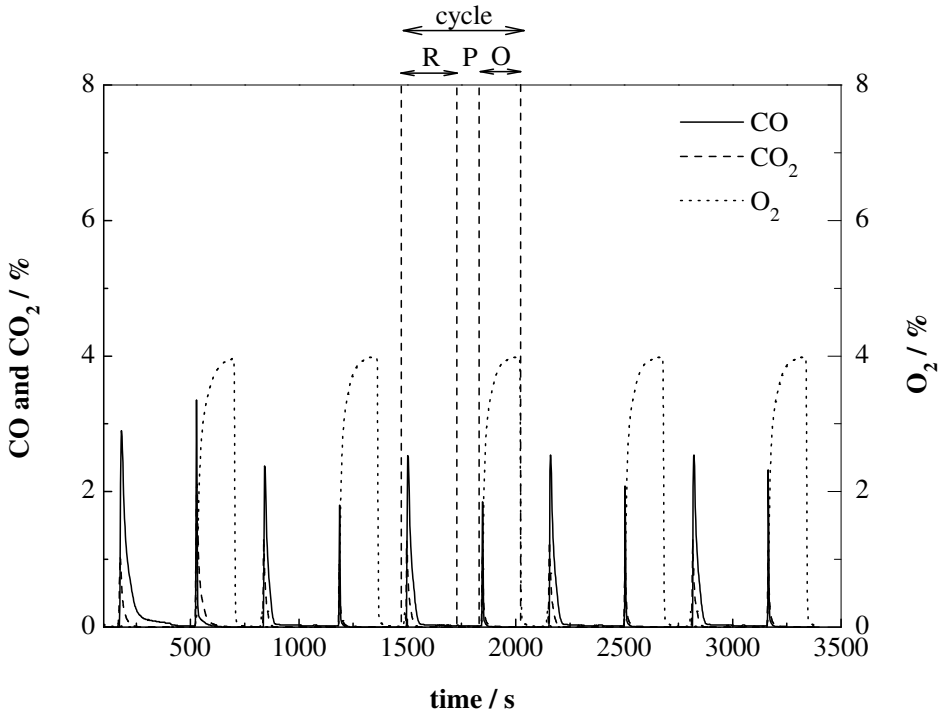
cycle
R
P
O
CO
CO2
O2
CO and CO2 / %
O2 / %
time / s
0
2
4
6
8
500
1000
1500
2000
2500
3000
3500

Fig. 6.

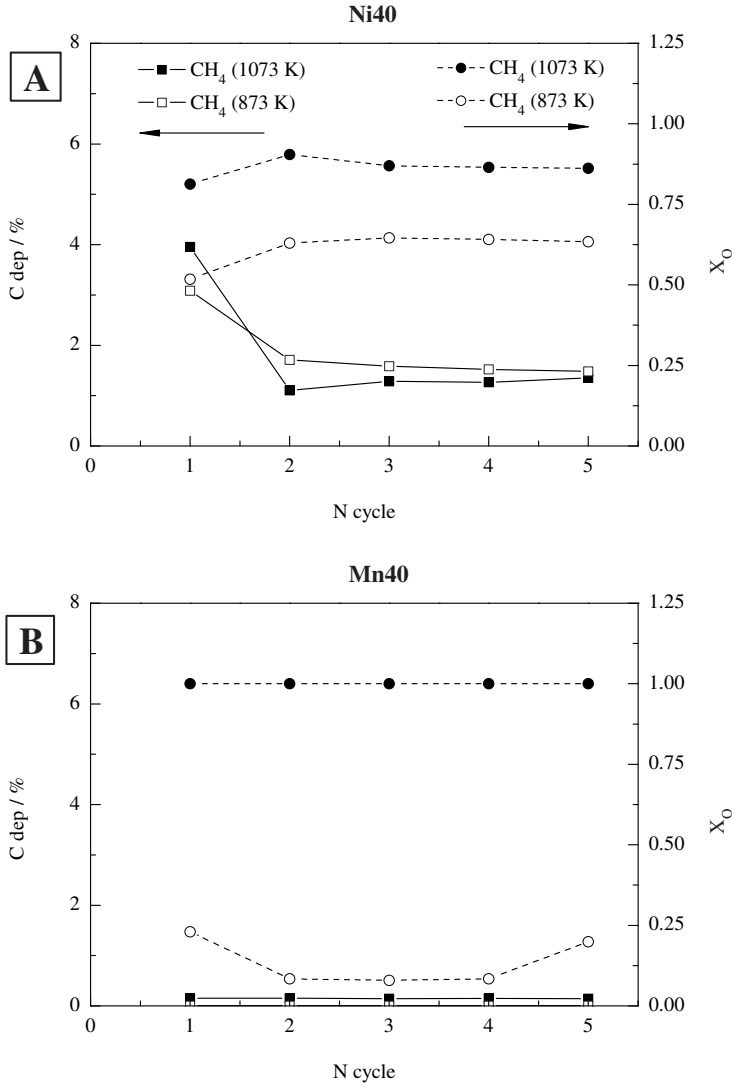
Ni40
A
CH4 (1073 K)
CH4 (873 K)
CH4 (1073 K)
CH4 (873 K)
C dep / %
X_O
N cycle
Mn40
B
C dep / %
X_O
N cycle

Fig. 7.

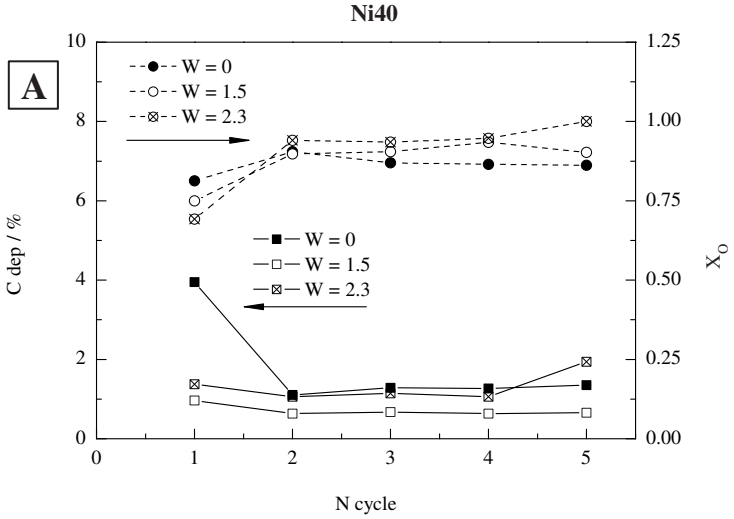
Ni40
A
W = 0
W = 1.5
W = 2.3
W = 0
W = 1.5
W = 2.3
C dep / %
X_O
N cycle
0
2
4
6
8
10
0.00
0.25
0.50
0.75
1.00
1.25
0
1
2
3
4
5

Fig. 8.

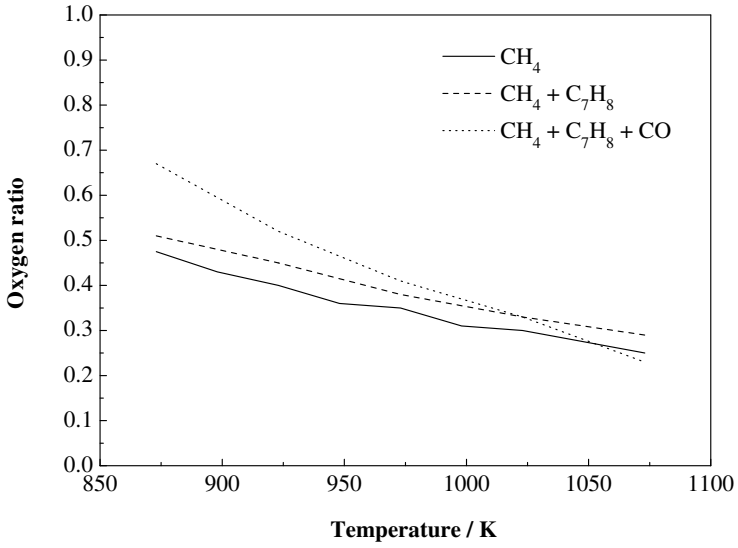
1.0
0.9
0.8
0.7
0.6
0.5
0.4
0.3
0.2
0.1
0.0
Oxygen ratio
850
900
950
1000
1050
1100
Temperature / K
CH4
CH4 + C7H8
CH4 + C7H8 + CO

Fig. 9.

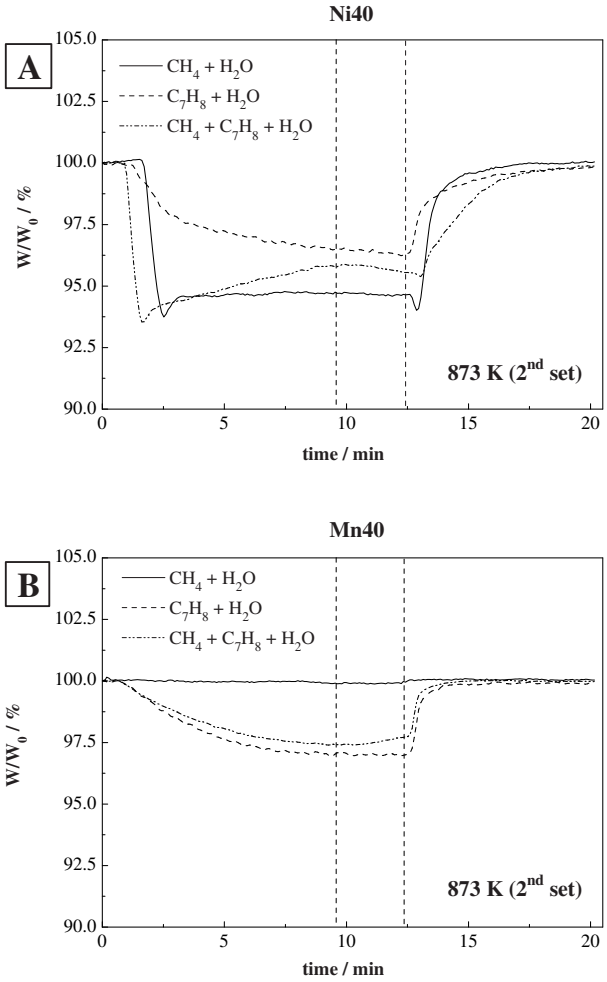
Ni40
A
CH4 + H2O
C7H8 + H2O
CH4 + C7H8 + H2O
W/W0 / %
873 K (2nd set)
time / min
Mn40
B
CH4 + H2O
C7H8 + H2O
CH4 + C7H8 + H2O
W/W0 / %
873 K (2nd set)
time / min

Fig. 10.

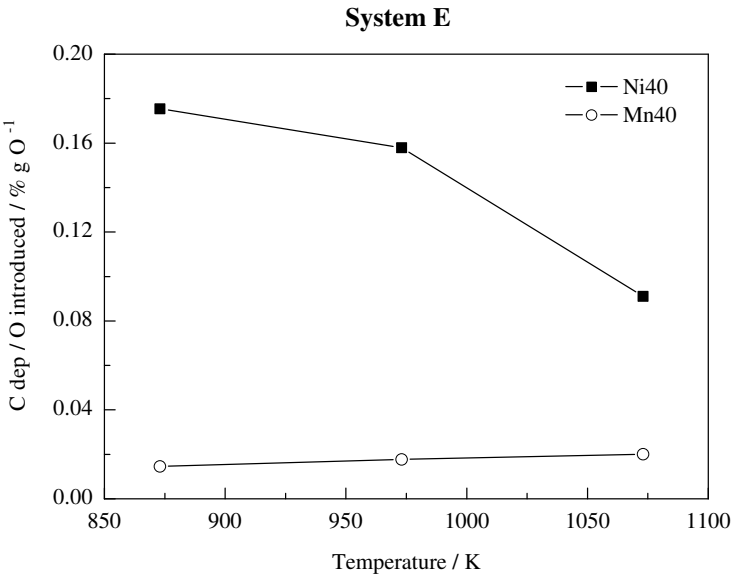
System E
Ni40
Mn40
C dep / O introduced / % g O -1
0.20
0.16
0.12
0.08
0.04
0.00
850
900
950
1000
1050
1100
Temperature / K

Fig. 11.